ISSN 1063-7729, Astronomy Reports, 2015, Vol. 59, No. 1, pp. 72–87. © Pleiades Publishing, Ltd., 2015.
Original Russian Text © A.A. Zlenko, 2015, published in Astronomicheskii Zhurnal, 2015, Vol. 92, No. 1, pp. 80–96.

A Celestial-Mechanical Model for the Tidal Evolution of the Earth–Moon System Treated as a Double Planet

A. A. Zlenko*

Moscow Automobile and Roadway State Technical University, Moscow, Russia

Received May 6, 2014; in final form, May 21, 2014

Abstract—A celestial-mechanical model for the motion of two viscoelastic spheres in the gravitational field of a massive point is considered, treating them as a double planet. The spheres move along quasi-circular orbits in a single plane, with their rotational axes perpendicular to this plane. The deformation of the spheres is described using the classical theory of small deformations. A Kelvin–Voigt model is adopted for the viscous forces. A system of evoutionary equations is obtained and applied to analyze the joint translational–rotational tidal evolution of the Earth and Moon in the gravitational field of the Sun. This system has been numerically integrated several billion years into the past and into the future. The results are compared with the predictions of other theories, paleontological data, and astronomical observations.

DOI: 10.1134/S1063772915010096

1. INTRODUCTION

The theory of tides originated with work by Newton and Laplace. The main achievements in this area were collected, systematized, and analyzed by Darwin [1], and further developed by MacDonald [2], who studied the evolution of the Earth–Moon system without including the influence of the Sun. Goldreich [3] used the method of MacDonald to investigate the oblateness of the Earth and the influence of solar tides, but neglecting the ellipticity of the lunar orbit, and correctly averaged the equations of motion using three time scales.

The method of MacDonald was then used in various other studies. Beletskii [4] investigated the tidal evolution of the inclinations and rotations of celestial bodies. Webb [5] studied the evolution of the Earth–Moon system based on the ocean tides and compared his results with the model of Goldreich [3]. Krasinsky [6] combined the methods of MacDonald and Goldreich to reconstruct a dynamical history of the Earth–Moon system. Touma and Wisdom [7] developed various models for tidal phenomena in detail. It was shown that the evolution of the Earth–Moon system based on the models of Darwin–Mignard and Darwin–Cowley–Goldreich is essentially equivalent to that predicted by the model of Goldreich.

Efroimsky and Lainey [8] considered the effective dissipation function Q, which is proportional to the tidal frequency to the power α. They studied the tidal evolution of the Martian moon Phobos for $\alpha = 0.2$, 0.3, 0.4. Note that $\alpha = 0$ in the model of MacDonald and $\alpha = -1$ in the model of Mignard [9, 10]. The main distinguishing property of the approach proposed by Ferraz-Mello et al. [11] is that, in contrast to many studies based on the theory of Darwin, different coefficients are introduced for the harmonics of the tidal wave, instead of one Love number. A critical analysis of the mathematical formulas in the above theories describing the tidal moments, slowing of planetary rotation, and the delay angle, as well as the accuracy and range of applicability of the theories and connections with rheological models, are considered by Efroimsky and Williams [12] and Efroimsky and Makarov [13]. Note that the qualitative conclusions derived for the simpler MacDonald theory essentially remain correct [12].

The subsequent development of tidal theories is concerned with the creation of rheological models. Churkin [14–16] established a generalized theory of the Love number and applied it to the rheological models of Guk, Maxwell, Voigt, and others. His theory for the rotation of the inelastic Earth was applied to a Voigt model for the Earth's interior, and numerical estimates of rheological corrections to the precession, nutation, and axial rotation of the Earth were obtained. Efroimsky [17] introduced complex Love numbers as a function of the tidal frequency to study tides in the case of a rotational–orbital resonance between a planet and one of its satellites.

Vil'ke [18] developed a method for separating motions and averaging in systems with an infinite number of degrees of freedom, aimed at studying the motions of deformable bodies using a classical linear

*E-mail: zalaf121@mail.ru

elasticity theory for small deformations and a Kelvin–Voigt model for the viscous forces. This method was used to investigate the evolution of the orbital and rotational motions of a viscoelastic planet in a central Newtonian force field [19, 20]. The model for a celestial body of Markov and Minyaev [21] includes an isotropic, viscoelastic layer and a rigid core. A qualitative analysis of the motion of the moons of Mars is given, and the model parameters were refined based on the observations of the secular acceleration of Phobos. Vil'ke and Shatina [22] studied the tidal evolution of the motion of the Earth–Moon system in the gravitational field of the Sun, treating the Moon as a point mass.

Let us now turn to our model describing a double planet [23–25].

2. MATHEMATICAL MODEL FOR THE MOTION OF TWO VISCOELASTIC SPHERES IN THE GRAVITATIONAL FIELD OF A FIXED CENTRAL BODY

2.1. Formulation of the Problem

In the unperturbed motion, the barycenter C of the two uniform rigid spheres O_1 and O_2 with masses m_1 and m_2 moves in a circular, Keplerian orbit in a fixed plane in the gravitational field of a stationary massive point mass M. The spheres O_1 and O_2, in turn, move in circular Keplerian orbits about the barycenter C in the plane of its motion. The spheres rotate with specified constant angular speeds about axes passing through their centers of mass perpendicular to the plane of their orbital motion. All four motions are independent of each other. This formulation of the problem is possible because we have made the assumptions

$$m_2 \ll m_1 \ll M; \quad r_{i0} \ll R_2 \ll R_1, \qquad (1)$$

where r_{i0} ($i = 1, 2$) are the radii of the spheres, R_1 is the distance from the gravitating center to the barycenter, and R_2 is the distance between the centers of mass of O_1 and O_2 (we will further identify the names of the spheres with their centers of mass). These assumptions are satisfied, for example, by the Sun–Earth–Moon system.

In the perturbed motion, we treat the spheres as uniform, isotropic, viscoelastic bodies. Perturbations arise due to the deformation of the bodies in response to the centrifugal and gravitational forces. Since we are studying evolutionary motions, we assume that the centers of mass of the spheres move along quasi-circular orbits.

To describe the motion, we specify an inertial coordinate frame $OXYZ$ fixed to the gravitating center O, with the spheres moving in the OXY plane. We specify Koenig coordinate systems $O_iX_iY_i$ with the points O_i ($i = 1, 2$). The position of the barycenter C in the $OXYZ$ system is specified by the vector $\mathbf{R}_1 = \overrightarrow{OC}(R_1\cos\lambda_1,\ R_1\sin\lambda_1, 0)$, where $|\mathbf{R}_1| = R_1$, and λ_1 is the angle between $\mathbf{R}_1$ and the OX axis. The position of O_2 relative to O_1 in the $O_1X_1Y_1Z_1$ frame is specified by the vector $\mathbf{R}_2 = \overrightarrow{O_1O_2}(R_2\cos\lambda_2,\ R_2\sin\lambda_2, 0)$, where $|\mathbf{R}_2| = R_2$, and λ_2 is the angle between $\mathbf{R}_2$ and the OX_1 axis. The deformed state of the bodies is described by the classical theory of elasticity for small deformations. We adopted a Kelvin–Voigt model for the viscous forces, with the dissipation function $D_i[\dot{\mathbf{u}}_i]$ proportional to the elastic-force function $W_i[\dot{\mathbf{u}}_i]$, with the coefficient of proportionality χ_i (the viscosity coefficient):

$$D_i[\dot{\mathbf{u}}_i] = \chi_i W_i[\dot{\mathbf{u}}_i], \qquad (2)$$

where $\mathbf{u}_i(\mathbf{r}_i, t)$ is the shift in the points of the body O_i due to the deformations, $\dot{\mathbf{u}}_i = d\mathbf{u}_i/dt$ (here and below, a dot above a quantity denotes a time derivative), and $\mathbf{r}_i$ is the radius vector of the points in a sphere relative to the center O_i in the undeformed state.

The rotating spheres are associated with their own coordinate systems $O_iX_{ii}Y_{ii}Z_{ii}$, where the O_iZ_{ii} axis is perpendicular to the orbital plane (the O_iZ_i and O_iZ_{ii} axes coincide). The positions of the points in the viscoelastic sphere O_i in the $OXYZ$ coordinate system are determined by the vector field

$$\boldsymbol{\zeta}_i(\mathbf{r}_i, t) = \overrightarrow{OO}_i + \Gamma_i(\varphi_i)(\mathbf{r}_i + \mathbf{u}_i(\mathbf{r}_i, t)), \qquad (3)$$

where

$$\Gamma_i(\varphi_i(t)) = \begin{pmatrix} \cos\varphi_i & -\sin\varphi_i & 0 \\ \sin\varphi_i & \cos\varphi_i & 0 \\ 0 & 0 & 1 \end{pmatrix}. \qquad (4)$$

Here, Γ_i is the orthogonal operator for the translation from the Koenig coordinates $O_iX_iY_iZ_i$ to the coordinates $O_iX_{ii}Y_{ii}Z_{ii}$ and φ_i is the rotation of the $O_iX_{ii}Y_{ii}Z_{ii}$ system about the O_iZ_{ii} axis (φ_i is the angle between the O_iX_i and O_iX_{ii} axes).

In order to uniquely determine the positions of the centers of mass of the spheres O_i in the $O_iX_{ii}Y_{ii}Z_{ii}$ coordinate systems as the spheres move by $\boldsymbol{\zeta}_i(\mathbf{r}_i, t)$, we imposed the following conditions (relations) on this motion:

$$\int\limits_{V_i} \mathbf{u}_i dv_i = 0, \quad \int\limits_{V_i} \mathrm{curl}\mathbf{u}_i dv_i = 0 \qquad (5)$$

$$(dv_i = dx_{ii}dy_{ii}dz_{ii}),$$

where $V_i = \{|\mathbf{r}_i| < r_{i0}\}$ is the region occupied by O_i in the undeformed state.

The functional for the kinetic energy of the system has the form

$$T = \frac{1}{2}m\dot{\mathbf{R}}_1^2 + \frac{m_1m_2}{2m}\dot{\mathbf{R}}_2^2 + \frac{1}{2}\sum_{i=1}^{2}(J_i[\mathbf{u}_i]\dot{\varphi}_i^2 + 2G_i\dot{\varphi}_i + T_{0i}),$$

where

$$J_i[\mathbf{u}_i] = \int\limits_{V_i}[\mathbf{e}_3 \times (\mathbf{r}_i + \mathbf{u}_i)]^2\rho_i dv_i, \quad (6)$$

$$G_i = \int\limits_{V_i}[\mathbf{e}_3 \times (\mathbf{r}_i + \mathbf{u}_i), \dot{\mathbf{u}}_i]\rho_i dv_i,$$

$$T_{0i} = \int\limits_{V_i}(\dot{\mathbf{u}}_i)^2\rho_i dv_i,$$

$\mathbf{e}_3$ is the unit vector for the O_iZ_{ii} axis perpendicular to the OXY plane, and ρ_i is the density of the sphere O_i.

The potential energy associated with the gravitational interactions is given by

$$\Pi = \Pi_1 + \Pi_2 + \Pi_3, \quad (7)$$

where

$$\Pi_1 = -f\int\limits_{V_1}\{[\mathbf{R}_1 - (m_2/m)\mathbf{R}_2 + \Gamma_1(\mathbf{r}_1 + \mathbf{u}_1)]^2\}^{-1/2}\rho_1 dv_1$$

is the energy associated with the interaction between the gravitating center and the viscoelatic body O_1,

$$\Pi_2 = -f\int\limits_{V_2}\{[\mathbf{R}_1 + (m_1/m)\mathbf{R}_2 + \Gamma_2(\mathbf{r}_2 + \mathbf{u}_2)]^2\}^{-1/2}\rho_2 dv_2$$

is the energy associated with the interaction between the gravitating center and the viscoelatic body O_2,

$$\Pi_3 = -G\int\limits_{V_1}\int\limits_{V_2}\{[\mathbf{R}_2 + \Gamma_2(\mathbf{r}_2 + \mathbf{u}_2) - \Gamma_1(\mathbf{r}_1 + \mathbf{u}_1)]^2\}^{1/2}\rho_1\rho_2 dv_1 dv_2$$

is the energy associated with the deformable spheres O_1 and O_2, $f = GM$, G is the gravitational constant, and $m = m_1 + m_2$. Taking into account the condition (1) and neglecting terms of order $(R_2/R_1)^3(m_2/m)^3$ and higher order in smallness in the potential energy, and leaving only terms that are linear $\mathbf{u}_i$, we obtain

$$\Pi = -fm/R_1 - Gm_1m_2/R_2 + \Pi_p, \quad (8)$$

where

$$\Pi_p = \sum_{k=1}^{2}\sum_{i=1}^{2}f_{ki}/R_k^3\int\limits_{V_i}[\mathbf{r}_i\mathbf{u}_i - 3(\boldsymbol{\xi}_{ki}, \mathbf{r}_i)(\boldsymbol{\xi}_{ki}, \mathbf{u}_i)]\rho_i dv_i, \quad (9)$$

$$f_{1i} = f, \quad f_{2i} = Gm_{3-i},$$
$$\boldsymbol{\xi}_{ki} = \tau_{ki}[\cos(\lambda_k - \varphi_i), \sin(\lambda_k - \varphi_i), 0],$$
$$\tau_{21} = -1, \quad \tau_{ki} = 1 \quad (k \neq 2,\ i \neq 1).$$

Following [22], we introduced canonical Poincaré variables λ_k, Λ_k ($k = 1, 2$ to describe the motion of the barycenter and centers of mass O_i:

$$\Lambda_1 = m(fR_1)^{1/2}, \quad \Lambda_2 = m_r(f_0R_2)^{1/2}, \quad (10)$$

where $m_r = m_1m_2/m$, $f_0 = Gm$.

To describe the rotational motion of the bodies, we used the Andoyer canonical variables φ_i, I_i ($i = 1, 2$):

$$I_i = J_i[\mathbf{u}_i]\dot{\varphi}_i + G_i, \quad (11)$$

where $J_i[\mathbf{u}_i]$ and G_i is defined in (6).

The equation of motion was written in the form of the Routh equations

$$\dot{\Lambda}_k = -\frac{\partial\Re}{\partial\lambda_k}, \quad \dot{\lambda}_k = \frac{\partial\Re}{\partial\Lambda_k}, \quad \dot{I}_i = -\frac{\partial\Re}{\partial\varphi_i}, \quad (12)$$
$$\dot{\varphi}_i = \frac{\partial\Re}{\partial I_i}, \quad \frac{d}{dt}\nabla_{\dot{u}_i}\Re - \nabla_{u_i}\Re - \nabla_{\dot{u}_i}D_i = 0.$$

Here, $\Re$ is the Routh function, which has the form

$$\Re = -\frac{f^2m^3}{2\Lambda_1^2} - \frac{f_0^2m_r^3}{2\Lambda_2^2} + \sum_{i=1}^{2}\left\{\frac{I_i^2}{2A_i} - \frac{I_i^2}{2A_i^2}J_{i1}[\mathbf{u}_i] - \frac{I_i}{A_i}\left(\mathbf{e}_3, \int\limits_{V_i}(\mathbf{r}_i \times \dot{\mathbf{u}}_i)dv\right) + W_i[\mathbf{u}_i]\right\} + \Pi_p, \quad (13)$$

where $A_i = 0.4m_ir_{i0}^2$ is the moment of inertia of the undeformed sphere O_i,

$$J_{i1}[\mathbf{u}_i] = 2\int\limits_{V_i}[(\mathbf{r}_i, \mathbf{u}_i) - (\mathbf{e}_3, \mathbf{r}_i)(\mathbf{e}_3, \mathbf{u}_i)]\rho_i dv_i, \quad (14)$$

and an expression for Π_p is given by (9).

The equations of motion admit the integral of the angular momentum. When the Routh function (13) is written out in detail, it can be shown that the angular variables λ_k and φ_i appear in this function in the combination $\psi_{ki} = \lambda_k - \varphi_i$. It follows that

$$\dot{I}_i = -\frac{\partial\Re}{\partial\varphi_i} = -\sum_{k=1}^{2}\frac{\partial\Re}{\partial\psi_{ki}}\cdot\frac{\partial\psi_{ki}}{\partial\varphi_i} = \sum_{k=1}^{2}\frac{\partial\Re}{\partial\psi_{ki}}, \quad (15)$$

$$\dot{\Lambda}_k = -\frac{\partial \Re}{\partial \lambda_k} = -\sum_{i=1}^{2} \frac{\partial \Re}{\partial \psi_{ki}} \cdot \frac{\partial \psi_{ki}}{\partial \lambda_k} = -\sum_{i=1}^{2} \frac{\partial \Re}{\partial \psi_{ki}},$$

$$\dot{I}_1 + \dot{I}_2 + \dot{\Lambda}_1 + \dot{\Lambda}_2 = \sum_{i=1}^{2}\sum_{k=1}^{2} \frac{\partial \Re}{\partial \psi_{ki}} - \sum_{k=1}^{2}\sum_{i=1}^{2} \frac{\partial \Re}{\partial \psi_{ki}} = 0,$$

$$I_1 + I_2 + \Lambda_1 + \Lambda_2 = K_0 = \text{const}.$$

2.2. Finding the Displacements of Points in the Bodies due to their Deformation

The system (12) cannot be integrated in explicit form, since this is a quite complex system of differential equations. Therefore, we applied the method for separating motions in systems with an infinite number of degrees of freedom [18]. Since we assumed the rigidity of the elastic spheres O_i were high, we introduced the small parameters ε_i, proportional to the ratio of the squares of the angular velocity of rotation of a sphere at the initial time and of the lowest frequency for the intrinsic elastic vibrations of the sphere. The displacements $\mathbf{u}_i$ are small, and can be represented as a series in powers of ε_i:

$$\mathbf{u}_i(\mathbf{r}_i, t) = \varepsilon_i \mathbf{u}_{i1}(\mathbf{r}_i, t) + \varepsilon_i^2 \mathbf{u}_{i2}(\mathbf{r}_i, t) + \ldots, \quad (16)$$

$$\varepsilon_i = \rho_i r_{i0}^2 \dot{\varphi}_i^2(0)/E_i, \quad (17)$$

where E_i is the Young's modulus for the body O_i.

If $\varepsilon_i = 0$, then $\mathbf{u}_i(\mathbf{r}_i, t) = 0$, and the equations of the unperturbed motion follow from (12):

$$\dot{\Lambda}_1 = \dot{\Lambda}_2 = \dot{I}_1 = \dot{I}_2 = 0, \quad (18)$$

$$\dot{\lambda}_1 = \omega_1, \quad \dot{\lambda}_2 = \omega_2, \quad \dot{\varphi}_1 = \omega_3, \quad \dot{\varphi}_2 = \omega_4,$$

where

$$\omega_1 = \frac{f^2 m^3}{\Lambda_1^3}, \quad \omega_2 = \frac{f_0^2 m_r^3}{\Lambda_2^3}, \quad (19)$$

$$\omega_3 = \frac{I_1}{A_1}, \quad \omega_4 = \frac{I_2}{A_2}.$$

In this case, the center of mass of the two bodies C moves along a circular orbit about the fixed center O with a constant angular velocity ω_1, the bodies O_i move along circular orbits about their center of mass C with a constant angular velocity ω_2, and the bodies O_1 and O_2 rotate on their axes with constant angular velocities ω_3 and ω_4, normal to their orbital plane passing through their centers of mass.

It can be shown that, after the intrinsic vibrations of the viscoelastic spheres have died away, including only the first term $\varepsilon_i \mathbf{u}_{i1}$ in the expansion of $\mathbf{u}_i(\mathbf{r}_i, t)$ in powers of ε_i in (16), the last equations in (12) reduce to the two relations

$$\nabla_{u_i} W_i[\varepsilon_i \mathbf{u}_{i1} + \chi_i \varepsilon_i \dot{\mathbf{u}}_{i1}] \quad (20)$$

$$= \rho_i \Big\{ \omega_{2+i}^2 [\mathbf{r}_i - (\mathbf{e}_3, \mathbf{r}_i)\mathbf{e}_3] + \sum_{k=1}^{2} (f_{ki}/R_k^3)[3(\boldsymbol{\xi}_{ki}, \mathbf{r}_i)\boldsymbol{\xi}_{ki} - \mathbf{r}_i] \Big\} \quad (i = 1, 2),$$

where

$$\nabla_u W_i[\varepsilon_i \mathbf{u}] = -\frac{\rho_i r_{i0}^2 \dot{\varphi}_i^2(0)}{2(1+\nu_i)} \times \left(\frac{1}{1-2\nu_i} \nabla \operatorname{div} \mathbf{u} + \Delta \mathbf{u} \right), \quad (21)$$

and ν_i is the Poisson coefficient for the matter in the sphere O_i.

Equation (20) can be written in the form

$$\varepsilon_i \nabla_{u_i} W_i[\mathbf{u}_{i1} + \chi_i \dot{\mathbf{u}}_{i1}] \quad (22)$$

$$= \rho_i \left[\omega_{2+i}^2 (2\mathbf{r}_i/3 + B_0 \mathbf{r}_i) + \sum_{k=1}^{2} 3(f_{ki}/R_k^3) B_{ki} \mathbf{r}_i \right],$$

where

$$B_0 = \begin{pmatrix} 1/3 & 0 & 0 \\ 0 & 1/3 & 0 \\ 0 & 0 & -2/3 \end{pmatrix},$$

$$B_{ki} = \frac{1}{6} \begin{pmatrix} 3\cos 2\psi_{ki} + 1 & 3\sin 2\psi_{ki} & 0 \\ 3\sin 2\psi_{ki} & -3\cos 2\psi_{ki} + 1 & 0 \\ 0 & 0 & -2 \end{pmatrix}.$$

All the quantities in the right-hand side of (22) are calculated for the unperturbed motion.

Taking into account the fact that the stresses on the surfaces of the deformable bodies O_i are zero (i.e., the boundary conditions for the functions $\mathbf{u}_{i1}(\mathbf{r}_i, t)$ have the form $\sigma_{in} = 0$), with accuracy to within first-order terms in the small quantity χ_i, the solution of (22) has the form

$$\mathbf{u}_i(\mathbf{r}_i, t) \approx \varepsilon_i \mathbf{u}_{i1} = \mathbf{u}_{i11} + \mathbf{u}_{i12} + \mathbf{u}_{i13}, \quad (23)$$

$$\mathbf{u}_{i11} = \rho_i/E_i \omega_{2+i}^2 [-2/3(d_{i1}\mathbf{r}_i^2 + d_{i2} r_{i0}^2) + a_{i1}(B_0 \mathbf{r}_i, \mathbf{r}_i) + (a_{i1}\mathbf{r}_i^2 + a_{i2} r_{i0}^2) B_0] \mathbf{r}_i,$$

$$\mathbf{u}_{i12} = 3\rho_i/E_i \sum_{k=1}^{2} f_{ki} R_k^{-3} [a_{i1}(B_{ki}\mathbf{r}_i, \mathbf{r}_i)\mathbf{r}_i + (a_{i2}\mathbf{r}_i^2 + a_{i3} r_{i0}^2) B_{ki} \mathbf{r}_i],$$

$$\mathbf{u}_{i13} = -3\rho_i/E_i \sum_{k=1}^{2} f_{ki} R_k^{-3} \chi_i (\omega_k - \omega_{2+i}) \times \left[a_{i1} \left(\frac{\partial B_{ki}}{\partial \psi_{ki}} \mathbf{r}_i, \mathbf{r}_i \right) \mathbf{r}_i + (a_{i2}\mathbf{r}_i^2 + a_{i3} r_{i0}^2) \frac{\partial B_{ki}}{\partial \psi_{ki}} \mathbf{r}_i \right],$$

where

$$d_{i1} = \frac{(1+\nu_i)(1-2\nu_i)}{10(1-\nu_i)},$$
$$d_{i2} = -\frac{(3-\nu_i)(1-2\nu_i)}{10(1-\nu_i)},$$
$$a_{i1} = \frac{1+\nu_i}{5\nu_i+7}, \quad a_{i2} = -\frac{(1+\nu_i)(2+\nu_i)}{5\nu_i+7}.$$

The structure of $\mathbf{u}_i(\mathbf{r}_i, t)$ is such that the first term $\mathbf{u}_{i11}$ describes axially symmetrical, elastic deformation of the sphere O_i, which is compressed by the action of the centrifugal force associated with the rotation about the O_iZ_{ii} axis passing through the center of mass. The second term $\mathbf{u}_{i12}$ characterizes the deformation of the body O_i due to the external gravitational fields of the two other bodies. These fields also give rise to gravitational tides, given by the third term $\mathbf{u}_{i13}$, which contains the viscosity coefficient χ_i and influences the evolution of the motion.

2.3. Simplification and Averaging of the Equations of Motion

Let us write the canonical equations (12) in more detail, taking into account the Routh function and the displacements $\mathbf{u}_i(\mathbf{r}_i, t) \approx \varepsilon\mathbf{u}_{i1}$:

$$\dot{\Lambda}_k = 3\sum_{i=1}^{2}\rho_i f_{ki} R_k^{-3} \tag{24}$$
$$\times \int_{V_i}\left[\left(\frac{\partial\xi_{ki}}{\partial\lambda_k}, \mathbf{r}_i\right)(\boldsymbol{\xi}_{ki}, \varepsilon_i\mathbf{u}_{i1}) + (\boldsymbol{\xi}_{ki}, \mathbf{r}_i)\left(\frac{\partial\xi_{ki}}{\partial\lambda_k}, \varepsilon_i\mathbf{u}_{i1}\right)\right]dv_i,$$

$$\dot{\lambda}_k = \omega_k - 3\sum_{i=1}^{2}\rho_i f_{ki} R_k^{-4}\partial R_k/\partial\Lambda_k \tag{25}$$
$$\times \int_{V_i}\left[(\mathbf{r}_i, \varepsilon_i\mathbf{u}_{i1}) - 3(\boldsymbol{\xi}_{ki}, \mathbf{r}_i)(\boldsymbol{\xi}_{ki}, \varepsilon_i\mathbf{u}_{i1})\right]dv_i,$$

$$\dot{I}_i = 3\rho_i\sum_{k=1}^{2} f_{ki} R_k^{-3} \tag{26}$$
$$\times \int_{V_i}\left[\left(\frac{\partial\xi_{ki}}{\partial\varphi_i}, \mathbf{r}_i\right)(\boldsymbol{\xi}_{ki}, \varepsilon_i\mathbf{u}_{i1}) + (\boldsymbol{\xi}_{ki}, \mathbf{r}_i)\left(\frac{\partial\xi_{ki}}{\partial\varphi_i}, \varepsilon_i\mathbf{u}_{i1}\right)\right]dv_i,$$

$$\dot{\varphi}_i = \omega_{2+i} - 2\rho_i\frac{\omega_{2+i}}{A_i} \tag{27}$$
$$\times \int_{V_i}[(\mathbf{r}_i, \varepsilon_i\mathbf{u}_{i1}) - (\mathbf{e}_3, \mathbf{r}_i)(\mathbf{e}_3, \varepsilon_i\mathbf{u}_{i1})]dv_i$$
$$- \frac{\rho_i}{A_i}\left[\mathbf{e}_3, \int_{V_i}(\mathbf{r}_i \times \varepsilon_i\dot{\mathbf{u}}_{i1})dv_i\right].$$

Subsituting the resulting variables (23) into the equations of motion (24)–(27) and calculating the necessary cumbersome integrals yields the system of equations of motion

$$\dot{\Lambda}_k = -18\sum_{i=1}^{2}\rho_i^2/E_i D_{i2} m_{3-i}\omega_k^2/m \tag{28}$$
$$\times\{\chi_i(m_{3-i}/m)^{2k-3}\omega_k^2(\omega_k - \omega_{2+i}) + \omega_{3-k}^2[(-1)^{2-k}0.5\sin\tau + \chi_i(\omega_{3-k} - \omega_{2+i})\cos\tau]\},$$

$$\dot{I}_i = 18\rho_i^2/E_i D_{i2}\chi_i[\omega_1^4(\omega_1 - \omega_{2+i}) + (m_{3-i}/m)^2\omega_2^4(\omega_2 - \omega_{2+i}) + m_{3-i}/m\omega_1^2\omega_2^2(\omega_1 + \omega_2 - 2\omega_{2+i})\cos\tau], \tag{29}$$

$$\dot{\lambda}_k = \omega_k + 6\sum_{i=1}^{2}\rho_i^2/E_i D_{i2}(m_{3-i}/m)^{k-1} \tag{30}$$
$$\times\Lambda_k^{-1}\omega_k^2\{\omega_{2+i}^2 + 6(m_{3-i}/m)^{k-1}\omega_k^2 + 3(m_{3-i}/m)^{2-k}\omega_{3-k}^2[0.5 + 1.5\cos\tau + 3(-1)^{k-1}\chi_i(\omega_{3-k} - \omega_{2+i})\sin\tau]\},$$

$$\dot{\varphi}_i = \omega_{2+i} - 2\rho_i^2/E_i A_i^{-1}\omega_{2+i}[D_{i2}(\omega_1^2 + m_{3-i}/m\omega_2^2) + 2/3(2D_{i1} + D_{i2})\omega_{2+i}^2], \tag{31}$$

where

$$D_{i1} = \frac{8\pi r_{i0}^7(1-2\nu_i)(4-3\nu_i)}{525(1-\nu_i)},$$
$$D_{i2} = \frac{4\pi r_{i0}^7(1+\nu_i)(9\nu_i+13)}{105(5\nu_i+7)},$$
$$\tau = 2(\lambda_2 - \lambda_1).$$

The right-hand sides of these equations do not depend on φ_i. Since the equations (31) depend only on Λ_k and I_i, they can be separated from the remaining equations and integrated after the integration of (28)–(30). If $\omega_1 \neq \omega_2$, the angular variable τ is a rapid variable, and averaging Eqs. (28)–(30) over τ yields the evolutionary system of equations

$$\dot{\Lambda}_k = -18\omega_k^4\sum_{i=1}^{2}\chi_i\rho_i^2/E_i \tag{32}$$
$$\times D_{i2}(m_{3-i}/m)^{2k-2}(\omega_k - \omega_{2+i}),$$

$$\dot{I}_i = 18\chi_i\rho_i^2/E_i D_{i2}[\omega_1^4(\omega_1 - \omega_{2+i}) \tag{33}$$

$$+ (m_{3-i}/m)^2\omega_2^4\,(\omega_2 - \omega_{2+i})],$$

$$\dot\lambda_k = \omega_k + 6\Lambda_k^{-1}\omega_k^2 \times \sum_{i=1}^{2} \rho_i^2/E_iD_{i2}\left(\frac{m_{3-i}}{m}\right)^{k-1} \times [\omega_{2+i}^2 + (m_{3-i}/m)^{k-1}\omega_k^2 + 1.5(m_{3-i}/m)^{2-k}\omega_{3-k}^2]. \quad (34)$$

The right-hand sides of the averaged equations do not depend on λ_k, and Eq. (34) can be separated from (32)–(33) and integrated after the solution of the independent system (32)–(33).

Since

$$\Lambda_1 = \left(f^2m^3\omega_1^{-1}\right)^{1/3},$$
$$\Lambda_2 = \left(G^2m_1^3m_2^3m^{-1}\omega_2^{-1}\right)^{1/3},$$
$$\omega_3 = I_1/A_1, \quad \omega_4 = I_2/A_2,$$

the system (32)–(33) can be written in the more "intuitive" variables ω_j ($j = 1$–4):

$$\dot\omega_1 = c_1\omega_1^{16/3}\left[k_1(\omega_1 - \omega_3) + k_2(\omega_1 - \omega_4)\right], \quad (35)$$
$$\dot\omega_2 = c_2\omega_2^{16/3}[k_1\left(m_2/m\right)^2(\omega_2 - \omega_3) + k_2\left(m_1/m\right)^2(\omega_2 - \omega_4)],$$
$$\dot\omega_3 = c_3k_1[\omega_1^4\,(\omega_1 - \omega_3) + (m_2/m)^2\,\omega_2^4\,(\omega_2 - \omega_3)],$$
$$\dot\omega_4 = c_4k_2[\omega_1^4\,(\omega_1 - \omega_4) + (m_1/m)^2\,\omega_2^4\,(\omega_2 - \omega_4)],$$

where

$$k_i = \chi_i\rho_i^2/E_iD_{i2}, \quad c_1 = 54f^{-2/3}m^{-1}, \quad c_2 = 54G^{-2/3}m^{1/3}m_1^{-1}m_2^{-1}, \quad c_3 = 18A_1^{-1}, \quad c_4 = 18A_2^{-1}. \quad (36)$$

The system (35) has the first integral

$$3c_1^{-1}\omega_1^{-1/3} + 3c_2^{-1}\omega_2^{-1/3} + c_3^{-1}\omega_3 + c_4^{-1}\omega_4 = K_0. \quad (37)$$

Thus, we obtained the independent system of first-order ordinary differential equations (35) to investigate the evolution of the slow variables: the angular velocity of the orbital motion of the center of mass of the binary planet (two viscoelastic bodies) about the gravitating center ω_1, the angular velocity of the planets about their common center of mass ω_2, and the angular rotational velocities of the two bodies ω_3 and ω_4. The right-hand sides of these equations all contain the viscosity coefficient χ_i through the coefficients k_i. If χ_i is zero, there is no tidal evolution of the system.

3. NUMERICAL INTEGRATION OF THE EQUATIONS OF MOTION

3.1. Input Data

The system (35) was numerically integrated using the MATLAB R2013a programme package. We took the Sun to be the fixed gravitating center, the first body to be the Earth, and the second body to be the Moon. We took the following data from [26] for the current epoch:

—$G = 6.67428 \times 10^{-11}$ m^3 kg^{-1} s^{-2} is the gravitational constant,

—$f = GM_S = 1.32712442099 \times 10^{20}$ m^3/s^2 is the heliocentric gravitatonal constant,

—$GM_E = 3.986004418 \times 10^{14}$ m^3/s^2 is the geocentric gravitational constant,

—$M_M/M_E = 1.23000371 \times 10^{-2}$ is the ratio of the masses of the Moon M_M and the Earth M_E.

We also took the following quantities at the current epoch from [27]:

—the duration of a single orbit of the Earth–Moon system around the Sun, equal to a sidereal year, $T_1 = 365.25636296$ d, (38)

—the duration T_2 of a single orbit of the Moon about the Earth, equal to a sidereal month and also equal to the rotational period of the Moon T_4; i.e., $T_2 = T_4 = 27.3216616$ d,

—the duration of an Earth day $T_3 = 86\,400$ s,

—the radius of the Moon $r_{20} = 1737.4$ km,

—the radius of the Earth $r_{10} = 6371.032$ km.

We used the units of measurement

—for mass the solar mass $M = M_S = 1$, (39)

—for length $L = 10^8$ m,

—for time $T = 31\,558\,149.759744$ s, equal to one year.

In these new units

$$G = f = 1.321705528131173 \times 10^{11}, \quad (40)$$
$$m_1 = M_E = 3.003489616313853 \times 10^{-6},$$
$$m_2 = M_M = 3.694303371012516 \times 10^{-8},$$
$$m = 3.040432650023978 \times 10^{-6},$$
$$A_1 = 4.876471597254109 \times 10^{-9},$$
$$A_2 = 4.460588721066945 \times 10^{-12},$$

where A_i are the moments of inertia (13).

We find from (36) the values

$$c_1 = 6.844923013835195 \times 10^{-1}, \quad (41)$$
$$c_2 = 2.717213270640726 \times 10^{5},$$
$$c_3 = 3.691193446125189 \times 10^{9},$$
$$c_4 = 4.035341773382441 \times 10^{12}.$$

The initial values for ω_i were taken to be $\omega_i(0) = 2\pi/T_i$ $(i = 1{-}4)$, where we took T_i from (38). It follows [in the new units (39)]:

$$\omega_1(0) = \omega_{10} = 6.283185307179586, \quad (42)$$
$$\omega_2(0) = \omega_{20} = \omega_4(0) = \omega_{40} = 83.99831045063988,$$
$$\omega_3(0) = \omega_{30} = 2.294973413104126 \times 10^{3}.$$

We found k_1 from the second equation of (35) under the condition that the radius of the lunar orbit R_2 is increasing at the rate $\Delta R_{20} = 0.038$ m/yr at the current epoch [28]:

$$d\omega_{20} = c_2 k_1 \omega_{20}^{16/3} (m_2/m)^2 (\omega_{20} - \omega_{30})\, dt.$$

Assuming a time interval $dt = 1$ (in years) yields:

$$k_1 = d\omega_{20} / \left[c_2 \omega_{20}^{16/3} (m_2/m)^2 (\omega_{20} - \omega_{30})\right]. \quad (43)$$

Since $R_2 = \sqrt[3]{Gm\omega_2^{-2}}$, it follows that $dR_2 = -\frac{2}{3}\sqrt[3]{Gm\omega_2^{-5}}\, d\omega_2$. Since the time interval $dt = 1$ is very small on evolutionary scales, we have to a high degree of accuracy $dR_{20} = \Delta R_{20}$. Therefore,

$$d\omega_{20} = -1.5\sqrt[3]{G^{-1}m^{-1}\omega_{20}^{5}}\,\Delta R_{20}. \quad (44)$$

Substituting (44) into (43) yields

$$k_1 = -\frac{1}{36}\sqrt[3]{Gm^4\omega_{20}^{-11}}\, m_1 m_2^{-1} \quad (45)$$
$$\times \Delta R_{20} / (\omega_{20} - \omega_{30})$$

Calculations using (45) together with the data from (40) and (42) give

$$k_1 = 7.661095722418093 \times 10^{-24}. \quad (46)$$

We assumed in these calculations $\Delta R_{20} = 0.038\, L^{-1}$, where L is defined in (39).

We found k_2 from the condition that $d\omega_2/dt = d\omega_4/dt$ at the current epoch, since the orbital angular velocity of the Moon around the Earth is currently equal to the angular velocity of the Moon about its center of mass, and their two rates of variation are so close that we can take them to be equal. We find from the second and fourth equations of (35)

$$c_2 k_1 \omega_{20}^{16/3} (m_2/m)^2 (\omega_{20} - \omega_{30}) \quad (47)$$
$$= c_4 k_2 \omega_{10}^{4} (\omega_{10} - \omega_{40}).$$

Equation (47) together with the expressions (36) for c_2 and c_4 yield

$$k_2 = 3k_1 A_2 (m_2/m_1) \quad (48)$$
$$\times \sqrt[3]{G^{-2}m^{-5}\omega_{20}^{16}}\, (\omega_{20} - \omega_{30}) / (\omega_{10}^4(\omega_{10} - \omega_{40})).$$

Substituting all the required quantities from (40), (42), and (46) into (48) yields

$$k_2 = 2.546031240069387 \times 10^{-26}. \quad (49)$$

The value of the integral of the angular momentum K_0 (37) with the coefficients c_i (41) and the input data (42) is equal to (in the new units)

$$K_0 = 42.75292278673111. \quad (50)$$

The adequateness of the derived coefficients, in particular k_1, and of our model at the current epoch can be tested by finding the slowing of the Earth's rotation ΔT_{30}. The third equation of (35) yields

$$d\omega_{30} = c_3 k_1 [\omega_{10}^4 (\omega_{10} - \omega_{30}) \quad (51)$$
$$+ (m_2/m)^2 \omega_{20}^4 (\omega_{20} - \omega_{30})] dt.$$

Setting $dt = 1$ in (51) with the data (40)–(42) and (46) yields

$$d\omega_{30} = -5.604049652131884 \times 10^{-7}. \quad (52)$$

However, $T_3 = 2\pi/\omega_3$. Thus,

$$dT_{30} = -2\pi d\omega_{30}/\omega_{30}^2 T\ (s) \quad (53)$$

Substituting the value of $d\omega_{30}$ from (52) and T from (39) into (53), we find $dT_{30} = \Delta T_{30} \approx 0.002$ s/100 yr, in good consistency with astronomical observations [29].

3.2. Results of Numerical Integration and Analysis

1. Integration into the Past We integrated the system (35) with the input data (42) and the coefficients from (40), (41), (46), and (49) over time into the past from zero to -5 billion years using the ode45 software, designed to solve non-rigid systems of differential equations, with a relative error RelTol $= 10^{-13}$ and an absolute error AbsTol $= 10^{-15}$ (these errors did not change in the subsequent computations into the past and future). The following values of the angular variables were obtained for $t = -5$ billion years:

$$\omega_1 = 6.283149581125962, \quad (54)$$
$$\omega_2 = 3.704491483803059,$$
$$\omega_3 = 2.862809504155766 \times 10^{3},$$
$$\omega_4 = -3.740751844225381 \times 10^{7}.$$

The integral of the angular momentum was equal to

$$K_0 = 42.75292278673117.$$

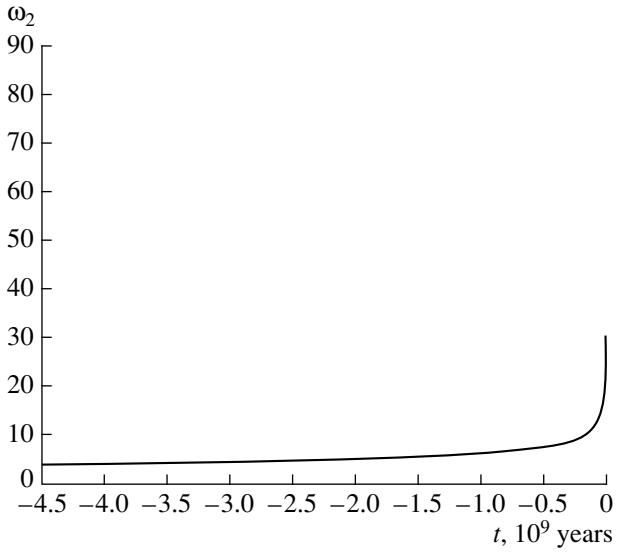

Fig. 1. Plot of the orbital angular velocity of the Moon ω_2 in the time interval from −4.5 billion years to zero.

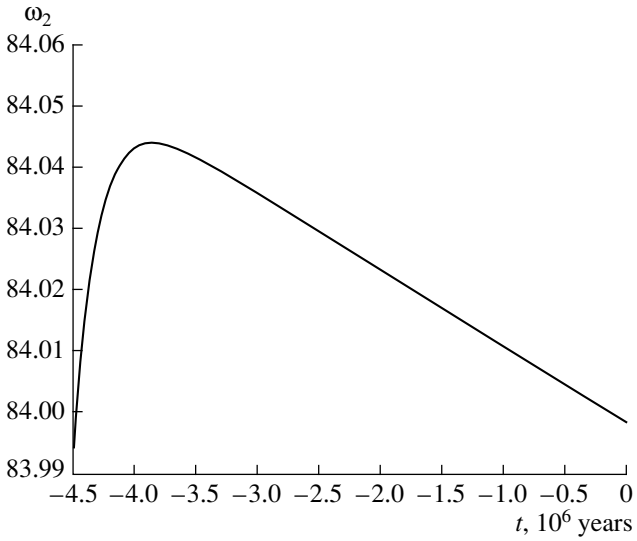

Fig. 3. Same as Fig. 1 for the time interval from −4.5 million years to zero.

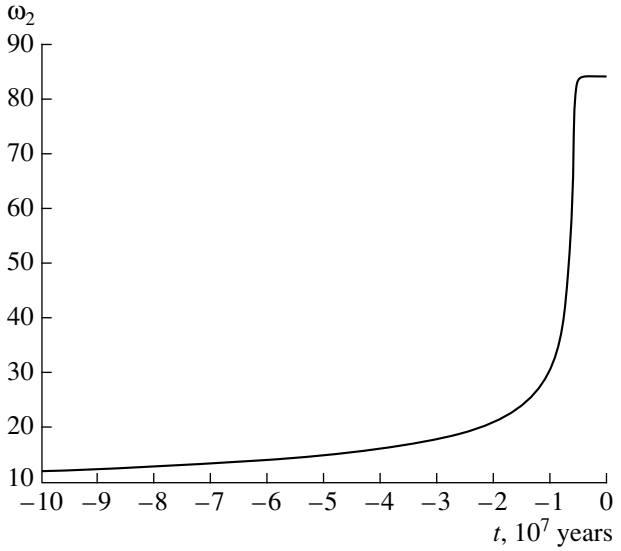

Fig. 2. Same as Fig. 1 for the time interval from −100 million years to zero.

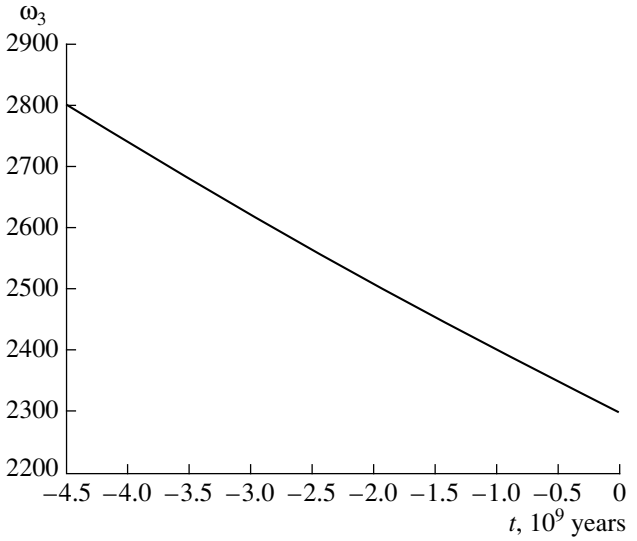

Fig. 4. Plot of the rotational angular velocity of the Earth ω_3 for the time interval from −4.5 billion years to zero.

We can see that this differs from the value of K_0 at $t = 0$ given by (50) by 6×10^{-14}.

As a test of the computations, the system (35) with the input data (54) was integrated from −5 billion years to zero. This yielded the following values at $t = 0$ after this reverse computation:

$$\omega_1 = 6.283185307179\mathbf{50},$$
$$\omega_2 = 8.399831045\mathbf{07062} \times 10^1,$$
$$\omega_3 = 2.29497341\mathbf{3103788} \times 10^3,$$
$$\omega_4 = 8.399831045\mathbf{06902} \times 10^1.$$

These differ from the original input data (42) in the digits indicated in bold. The computation from zero to −5 billion years occupied less than a minute on the Samsung NP510R5E laptop computer used.

Plots of the angular velocities for integration into the past in the time interval from 0 to −4.5 billion years are presented in Figs. 1–9. The horizontal axes plot the time and the vertical axes the angular variabiles (in the new units).

The orbital angular velocity of the Moon slowly increases in the time interval from −4.5 billion years to −100 million years (Fig. 1). It begins

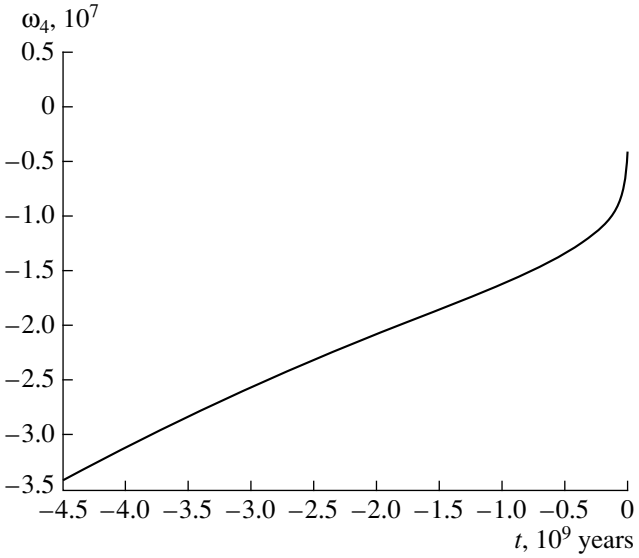

Fig. 5. Plot of the rotational angular velocity of the Moon ω_4 for the time interval from -4.5 billion years to zero.

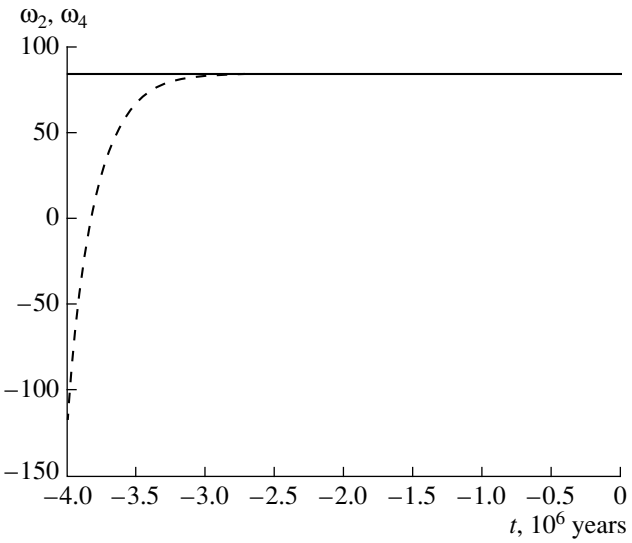

Fig. 7. Plot of the orbital ω_2 (solid curve) and rotational ω_4 (dashed curve) angular velocities of the Moon for the time interval from -4 million years to zero.

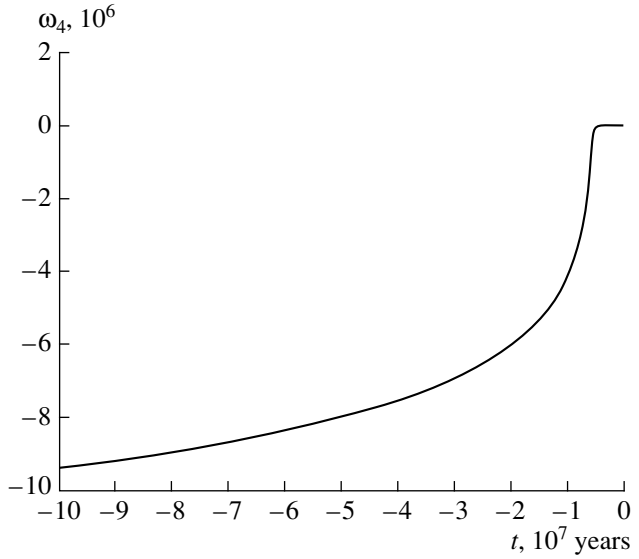

Fig. 6. Same as Fig. 5 for the time interval from -100 million years to zero.

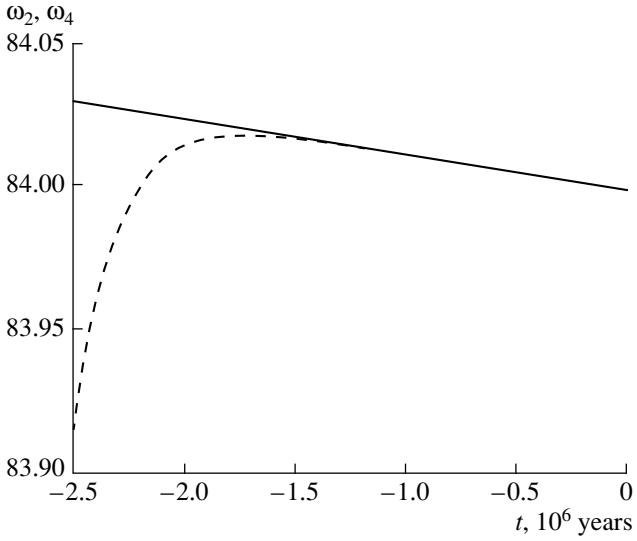

Fig. 8. Same as Fig. 7 for the time interval from -2.5 million years to zero.

to grow especially rapidly from -100 million years (Fig. 1) and from -10 million years (Fig. 2). At $t \approx -3.852728 \times 10^6$ years, ω_2 takes on its maximum value, $\approx$84.04385, then begins to decrease (Fig. 3), as is currently observed. The rotational angular velocity of the Earth ω_3 decreases almost linearly from $\omega_3 \approx 2.8005 \times 10^3$ to the current value (Fig. 4). The Moon displayed very rapid and reversed axial rotation 4.5 billion years ago. Further, over a very extended time, the (negative) rotational angular velocity of the Moon ω_4 gradually increased (Figs. 5, 6). At $t \approx -3.817$ million years, it changed sign, and the lunar axial rotation became prograde (Fig. 7). Figures 7 and 8 show that ω_4 begins to approach ω_2, with $\omega_4 \approx 83.9133$ and $\omega_2 \approx 84.0295$ at $t = -2.5$ million years. These two quantities have essentially become equal at $t = -1$ million years: $\omega_2 \approx 84.0108$, $\omega_4 \approx 84.0107$. This represents a 1 : 1 lunar spin–orbital resonance, when the lunar "day" is equal to a lunar month. This resonance is preserved in the future, although the

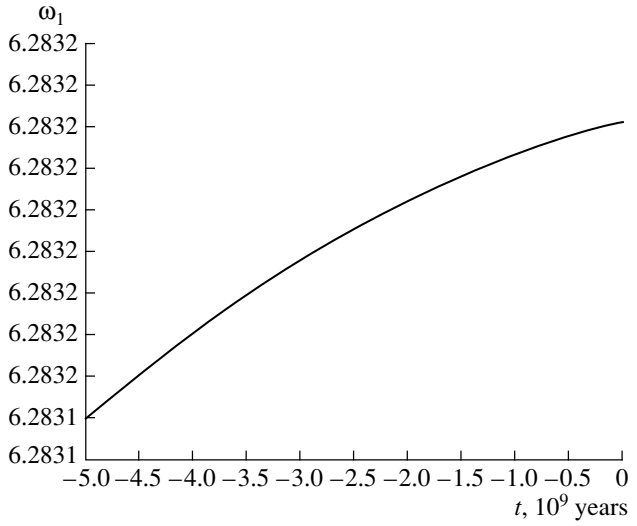

Fig. 9. Plot of the angular velocity of the Earth–Moon barycenter in its motion about the Sun ω_1 for the time interval from −5 billion years to zero.

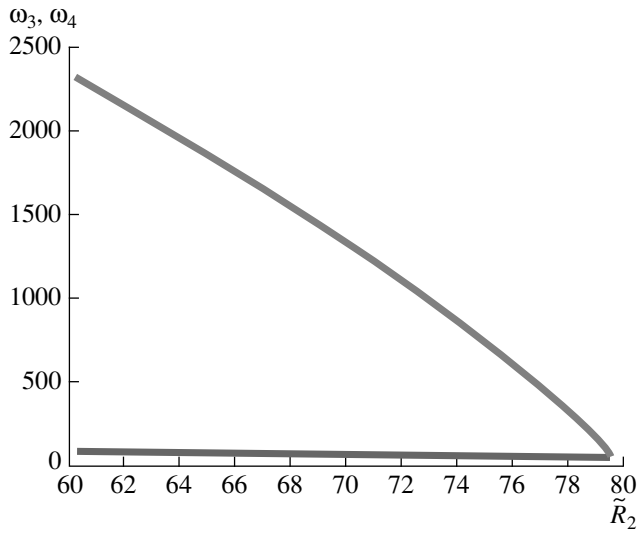

Fig. 10. Rotational angular velocities of the Earth ω_3 (upper) and the Moon $\omega_4 = \omega_2$ (lower) as the Moon recedes from the Earth, as a function of the distance between the Moon and Earth (in Earth radii).

values of the angular variables change: $\omega_2 = \omega_4$ with accuracy to within 2–4 digits after the decimal point; i.e., the phenomenon of libration is observed. At $t \approx -1.7330$ million years, ω_4 reaches its maximum value of 84.017 and then decreases to the current value (Fig. 8). The value ω_1 changes almost linearly, growing by $\approx 3.57 \times 10^{-5}$ from $t = -5$ billion years to $t = 0$ (Fig. 9).

2. Integration into the Future Predicting the evolution of the Earth–Moon system into the future is even more difficult—both because we do not know the intrinsic time frame, and because the values obtained could be erroneous due to imperfections in our model. Therefore, we adopted the distance between the Moon and the Earth, taken to vary within some reasonable limits, as an independent variable (we discuss this question further in Section 5).

We obtained the following system of equations of motion from (35):

$$\omega_1' = c_1\omega_1^{16/3}\left[k_1(\omega_1-\omega_3)+k_2(\omega_1-\omega_4)\right]V, \quad (55)$$
$$\omega_2' = -1.5(Gm)^{0.5}(\tilde{R}_2)^{-2.5}(\tilde{r}_{10})^{-1.5},$$
$$\omega_3' = c_3k_1[\omega_1^4(\omega_1-\omega_3)+(m_2/m)^2\omega_2^4(\omega_2-\omega_3)]V,$$
$$\omega_4' = c_4k_2[\omega_1^4(\omega_1-\omega_4)+(m_1/m)^2\omega_2^4(\omega_2-\omega_4)]V,$$

where $\omega_i' = d\omega_i/d\tilde{R}_2$ $(i = 1–4)$, $\tilde{R}_2$ is the distance between the centers of mass of the Earth and Moon in Earth radii, $\tilde{r}_{10}$ is the Earth radius in the new units,

$$V = c_5\tilde{R}_2^{5.5}/[k_1(m_2/m)^2(\omega_2-\omega_3) \quad (56)$$
$$+ k_2(m_1/m)^2(\omega_2-\omega_4)],$$
$$c_5 = (-1/36)G^{-1.5}m^{-2.5}m_1m_2\tilde{r}_{10}^{6.5},$$

$$\tilde{r}_{10} = 0.06371032.$$

The system (55) with the initial data (42) and $\tilde{R}_2(t=0) = 60.390210643874219$ in units of the Earth radius was integrated into the future using the ode23t software, designed for the computation of moderately rigid systems. The integration was ceased when $\tilde{R}_2 = 79.530836093424753$, with a report that *it is not possible to achieve the required accuracy without reducing the integration step below the lowest allowed value*, equal to 2.825503×10^{-13}. Physically, this is due to qualitative variations in the motion of our system. The rotational angular velocity of the Earth ω_3 decreases, remaining larger than $\omega_2 = \omega_4$, then approaches these values, indicating a passage through the resonance point $\omega_2 = \omega_3 = \omega_4$ (Fig. 10). The integration was stopped during this approach. The passage through this resonance point using the system (35) shows that the distance between the Moon and the Earth achieves its maximum at that time, equal to 506 692 km, and further monotonically decreases. The values of ω_2 and ω_4 are very close, and appear as a single solid curve in Fig. 11.

In order to carry the integration of the system (55) further, we used the system (35) to obtain new data for $\tilde{R}_2 = 79.530790508689833$ (near, but beyond, the resonance point):

$$\omega_1 = 6.283183444133909, \quad (57)$$
$$\omega_2 = 55.579856169772796,$$
$$\omega_3 = 55.128835732831654,$$

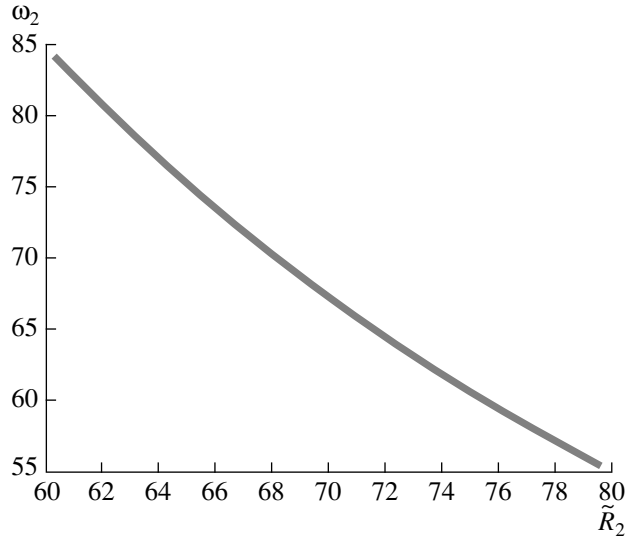

Fig. 11. Plot of the orbital angular velocity of the Moon ω_2 as the Moon recedes from the Earth, as a function of the distance between the Moon and Earth (in Earth radii).

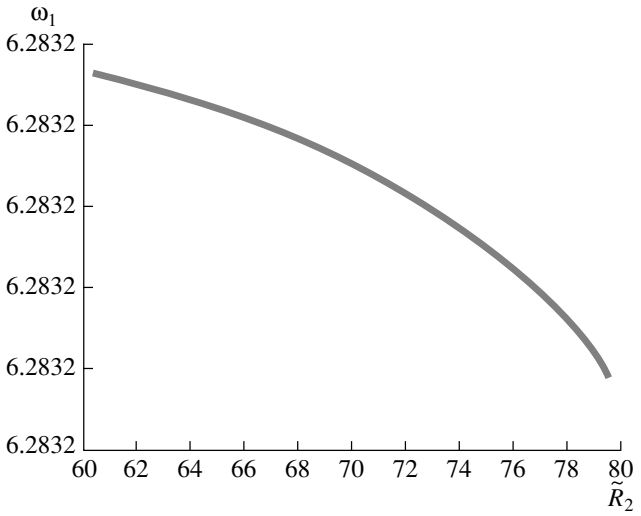

Fig. 12. Plot of the angular velocity ω_1 of the barycenter of the Earth–Moon system as the Moon recedes from the Earth, as a function of the distance between the Moon and Earth (in Earth radii).

$$\omega_4 = 55.571553739447416.$$

The corresponding integral of the angular momentum,

$$K_0 = 42.75292278673107,$$

differs by 4×10^{-14} from the initial value (50). Here, we can see that ω_3 is now smaller than ω_2.

The following values of the angular variables were obtained when $\tilde{R}_2 = 79.530836093424753$:

$$\omega_1 = 6.283183446070644, \qquad (58)$$

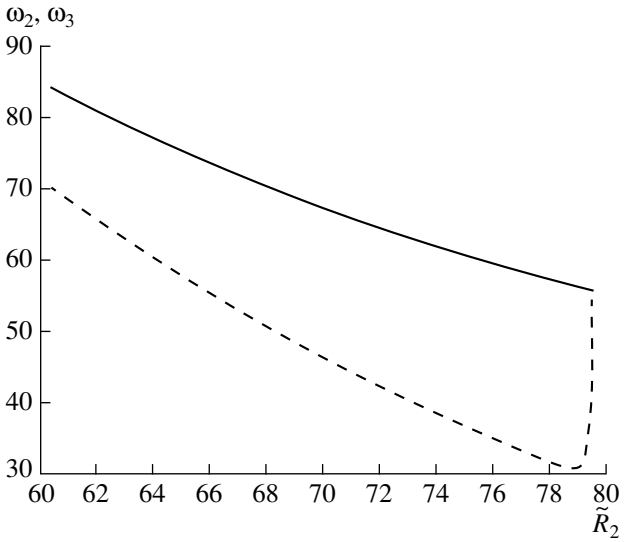

Fig. 13. Plot of the rotational angular velocity of the Earth ω_3 (dashed curve) and the orbital angular velocity of the Moon ω_2 (solid curve) as the Moon approaches the Earth from 79.53 to 60.39 Earth radii.

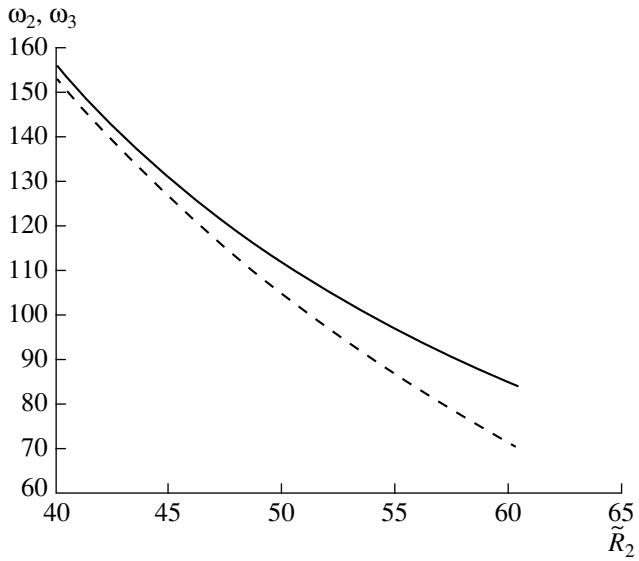

Fig. 14. Same as Fig. 13 as the Moon approaches the Earth from 60.39 to 40 Earth radii.

$$\omega_2 = 55.579808373540935,$$
$$\omega_3 = 56.02657531218837,$$
$$\omega_4 = 55.571559310581840.$$

The corresponding integral of the angular momentum,

$$K_0 = 42.75292278673108,$$

differs by 3×10^{-14} from the initial value (50). The

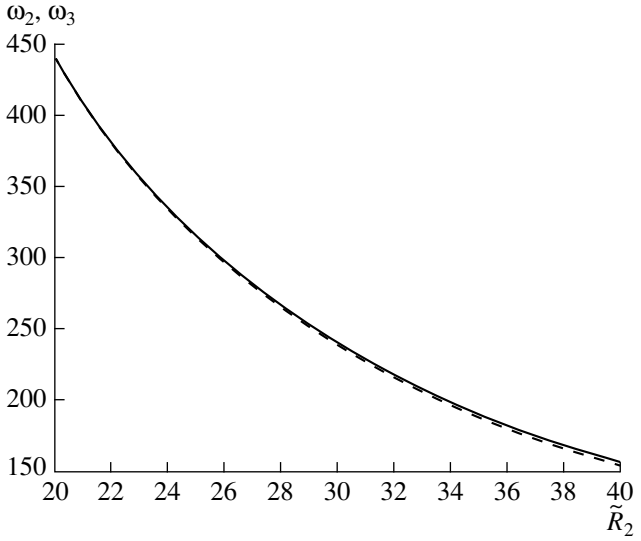

Fig. 15. Same as Fig. 13 as the Moon approaches the Earth from 40 to 20 Earth radii.

angular velocity ω_1 decreased by $\approx 2 \times 10^{-6}$ compared to the initial value (42) (Fig. 12).

We integrated the system (55) with the initial data (58) as $\tilde{R}_2$ varied from 79.530790508689833 to unity; i.e., as the Moon approached the Earth. Figures 13–17 show plots of the variations of ω_2 and ω_3. In Fig. 13, ω_3 sharply decreases, reaching its minimum value $\omega_3 \approx 30.668$ when $\tilde{R}_2 \approx 78.854$. At this time, $\omega_2 \approx 56.297$. Further, ω_3 begins to grow, remaining smaller than ω_2.

We observe the same picture in Fig. 14. In Fig. 15, ω_2 and ω_3 begin to approach each other, and we have $\omega_2 \approx 440.7$ and $\omega_3 \approx 440.6$ when $\tilde{R}_2 = 20$. We observe here the resonance $\omega_2 : \omega_3 : \omega_4 \approx 1 : 1 : 1$, when the Earth and Moon both keep the same face toward each other. The angular velocities ω_2 and ω_3 grow, but remain equal. This continues roughly until $\tilde{R}_2 = 10$, after which ω_2 and ω_3 begin to diverge and increase, but with ω_2 growing appreciably faster: we have when $\tilde{R}_2 = 5$ $\omega_2 \approx 3525$ and $\omega_3 \approx 2352$ (Fig. 16), and $\omega_2 \approx 39\,420$ and $\omega_3 \approx 3800$ when $\tilde{R}_2 = 1$ (Fig. 17). The Moon rapidly approaches the Earth, and collides with it when $\tilde{R}_2 = 1$. At that time, $K_0 = 42.75292278672882$, which differs from the initial value by 229×10^{-14}. The angular velocity of the barycenter of the Earth–Moon system ω_1 decreases by $\approx 10^{-5}$ compared to the initial value (42) (Fig. 18).

Further, to compute the distance of the Earth–Moon barycenter from the Sun R_1, the distance from the Earth to the Moon R_2, and the current periods of rotation of the Earth and Moon T_t (for the current rotational angular velocity ω_t), we applied the following formulas:

$$R_1 = \sqrt[3]{GM\omega_1^{-2}}L \text{ m}, \quad R_2 = \sqrt[3]{Gm\omega_2^{-2}}L \text{ m}, \quad (59)$$
$$T_t = 2\pi/\omega_t T \text{ s},$$

where the values of the constants are given in (39), (40). We used the resulting plots of the variations of the angular velocities to construct the tidal evolution of the system on cosmological time intervals.

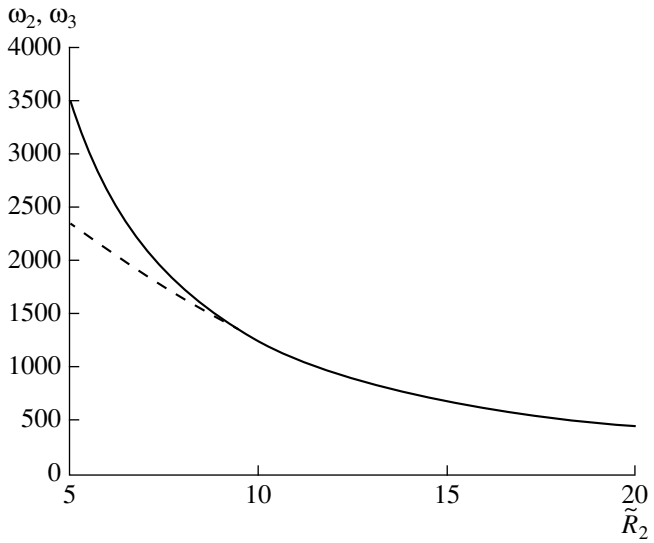

Fig. 16. Same as Fig. 13 as the Moon approaches the Earth from 20 to 5 Earth radii.

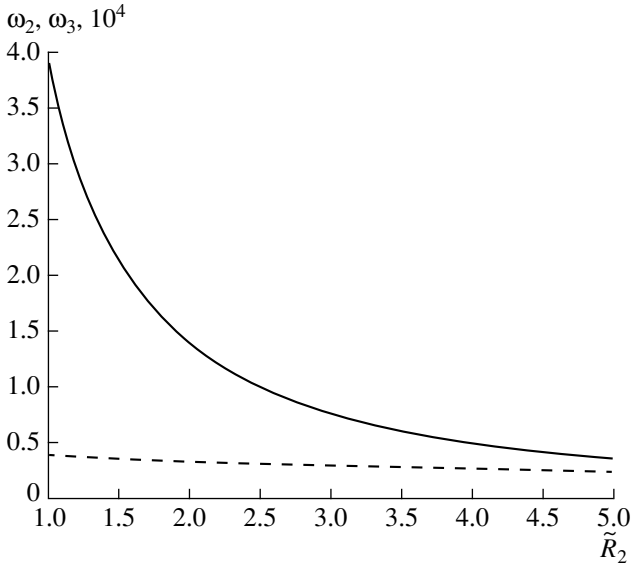

Fig. 17. Same as Fig. 13 as the Moon approaches the Earth from 5 to 1 Earth radii.

4. TIDAL EVOLUTION OF THE EARTH–MOON SYSTEM

4.5 billion years ago, the distance between the Moon and the Earth was three million kilometers. The Moon then slowly approached the Earth over a long time interval. 500 million years ago, the Earth–Moon distance was 1.9 million kilometers. An interval of more rapid variation of the parameters of motion of the Moon began about 100 million years ago. The Moon reached its minimum distance to the Earth about 3.9 million years ago, with this distance differing from the distance at the current epoch by about 150 km. The Moon then began to slowly recede, as is observed today.

An Earth day 4.5 billion years ago was only a few hours shorter than the current day, 19.667 hr. Our theory agrees with all other existing theories that the duration of the day was shorter in the past due to the effect of tidal friction, and the length of the day has gradually increased over the course of the Earth's evolution. This is confirmed by paleontological data: the duration of an Earth day was 21.9 hr 620 million years ago [30].

The Moon displayed very rapid and retrograde rotation 4.5 billion years ago. The rotational velocity of the Moon then gradually slowed, until the direction of the rotation was reversed 3.8 million years ago; i.e., the rotation direction became the same as at the current epoch. The Moon's rotation rate then began to increase, and the length of the lunar "day" to shorten. About 1.733 million years ago, the duration of the lunar "day" reached a local minimum, differing from the value for the current epoch by several minutes. The lunar "day" then began to gradually increase.

The modern history of the Moon begins roughly one million years ago, when its orbital angular velocity became essentially equal to its rotational velocity. The length of the lunar "day" became equal to the length of a lunar month; i.e., a 1 : 1 resonance was achieved. The computations indicate that this resonance has been preserved over the entire evolution of the Moon.

Laser observations indicate that the Moon is currently receding from the Earth [28]. In the future, the duration of the Earth day and the lunar month (lunar day) will smoothly grow, but the Earth day will remain shorter than the month. At a distance of about 506 692 km—the maxinum distance between the Moon and the Earth —they will become comparable and equal to 41.29 d. Further, the Moon will begin to gradually approach the Earth, and the lunar day will begin to decrease while the Earth day increases. At an Earth–Moon distance of 502 380 km, the rotation period of the Earth will reach its maximum value of 74.8 d and the rotational period of the Moon will be 40.8 d, after which the Earth day will begin to decrease, remaining longer than a lunar month. The motion of the Moon back toward the Earth can be explained by tidal theory [1, 31]: since the month is shorter than the rotational period of the Earth, the effect of tidal friction begins to draw the Moon back toward the Earth. Our results are also supported by other theories [2, 3]. Goldreich [3] has written that, since the lunar tidal torque exceeds the solar tidal torque at a maximum distance of 75 Earth radii, and since the Moon's orbital moment of inertia exceeds the Earth's, the rotation of the Earth will begin to be accelerated while the Moon approaches the Earth, with the Earth day always remaining slightly longer than the month.

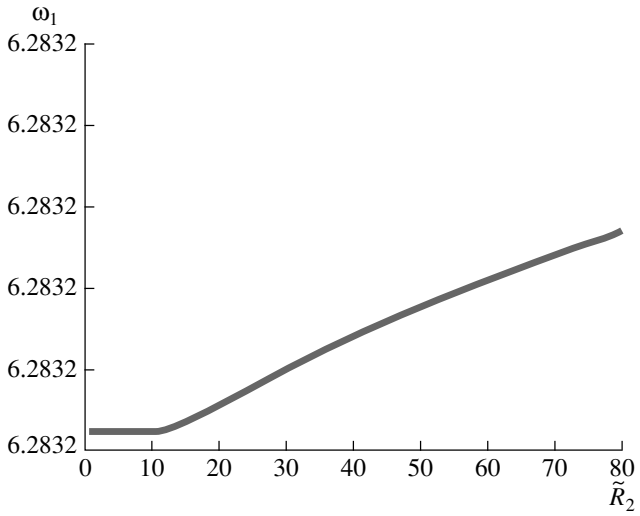

Fig. 18. Plot of the angular velocity of the barycenter of the Earth–Moon system ω_1 as the Moon approaches the Earth from 79.53 to 1 Earth radii.

The approach of the Moon toward the Earth and the increase in the Earth's rotation rate will mean that the Earth day and the lunar month approach each other and decrease sharply. They both become equal to about 5.21 d at a distance of about 20 Earth radii. This testifies to synchronization of the motions; i.e., $\omega_2 \approx \omega_3 \approx \omega_4$, so that the Earth and the Moon keep their same faces toward each other. However, although the angular velocities are equal, they are not constant, and increase. This synchronization is unstable, and becomes disrupted at distances of less than 10 Earth radii. As before, ω_2 is equal to ω_4. The Moon approaches the Earth, its orbital velocity appreciably exceeds the rotational velocity of the Earth; ultimately, the Moon passes inside the Roche limit at a distance of less than three Earth radii, is disrupted, and collides with the Earth.

During this expansive evolution, the radial distance of the barycenter of the Earth–Moon slowly

increases, increasing by ≈ 224 km by the end of the evolution, compared to its value at $t = 0$.

5. DISCUSSION AND CONCLUSION

The evolutionary picture described above is hypothetical, and we do not know exactly to what points in the past and the future it is correct. We have considered the evolution only of the four angular velocities characterizing the distance between the barycenter of the Earth–Moon system and the Sun and between the Moon and the Earth, and the axial rotations of the Earth and the Moon. Let us consider the basis for the applicability of our model.

Cosmological time intervals of several billion years are rather long for studies of the evolution of the Earth–Moon system. Therefore, it is unlikely that all the variables changed in a continuous fashion during the evolution of this system. It is known from paleontological data that there have been several epochs of mass extinction on the Earth in the past. This suggests that the tilt of the Earth's axis could experience jumps, possibly including a reversal of the poles. This could lead to changes in the direction and rate of the Earth's rotation. This means that, however accurate a model may be, we cannot be confident of the correctness of our results further than 12 000 years in the past (the epoch of the latest catastrophe, the worldwide flood). If we consider a time interval of 4.5 billion years, the mean position of the Earth's axis has been perpendicular to its orbital plane.

Another theoretical basis is the fact that, in the motion of the center of mass of a viscoelastic planet in a central force field, its rotational axis will tend to become oriented perpendicular to its orbital plane [20]. In relation to this reasoning, the Moon's rotation axis is also assumed to be perpendicular to the plane of its orbit. Since the Earth's equator could unpredictably change its position, the angle between the Moon's orbital plane and the Earth's equator could also vary unpredictably. The mean value of this angle is taken to be zero.

It is known that the limiting motion of the center of mass of a viscoelastic planet in a central force field is circular [19]. Therefore, in our model, the barycenter of the Earth–Moon system moves around the Sun in a quasi-circular orbit over cosmological time intervals, and the Moon likewise moves about the Earth in a quasi-circular orbit; i.e., along winding or unwinding spirals.

On the one hand, our celestial mechanical model is simple in the sense that it has relatively few parameters, due to the difficulty of the problem that we wish to solve. On the other hand, it can be considered complex. A Kelvin–Voigt model has been adopted for viscous forces. The bodies are spheres in their unperturbed motion, and compressed along their rotational axes in their perturbed motion, with their surfaces taking on complex shapes due to the action of viscous, dissipative forces. Naturally, the shapes of the bodies are continually changing as the parameters of their motion change. The influence of the oceans on the surface of the Earth has not been taken into account at all. The study of Krasinsky [32] casts doubt on the hypothesis that the main contribution to the tidal dissipation of the Earth is made by the oceans.

Let us now consider the time scales for the evolution of the Earth and Moon. The coefficients k_1 and k_2 from (36), which appear in the equations of motion, are integrated coefficients characterizing the viscoelastic properties of the Earth and Moon. We calculated their values at the current epoch, based on available astronomical data. However, their values will change with time in reality, and in ways that are not known. This could not only disrupt the chronology, but also provide the main reason for discrepancies between the model and physical reality. In other theories, lack of knowledge of the true variations in the dissipative function Q associated with the time-dependent delay angle, the relative angular velocity of the rotations of celestial bodies, and other factors have made it necessary to assume that the delay angle is constant in a first approximation. As was shown in [2], the epoch of the maximally close approach of the Moon to the Earth occurred 1.79 billion years ago, when this distance was 2.72 Earth radii. This means that the Moon was inside the Roche lobe, and subject to disruption. Such a short "lifetime" for the Moon is in contradiction with available paleontological data [33] and the results of lunar expeditions. It is noted in the later work of Kaula [34] concerning dynamical aspects of the origin of the Moon that, if the rate of recession of the Moon from the Earth has been constant throughout its history, the Moon should have been dangerously close to the Earth only 1.75 billion years ago. Krasinsky [6] suggests that Q must have grown with time in the past.

Integrating into the past, we restricted our analysis based on available data on the ages of the Earth and Moon, 4.5 billion years. In this case, we do not encounter the problem of the small time scale for the evolution of the lunar orbit, which the theories indicated above cannot resolve. The minimum distance between the Moon and Earth is only about 150 km smaller than their current separation. It follows from the evolution of our system that the origin of the Moon may not be related to the Earth, and it is quite likely that it formed in another region of circum-solar space.

For this reason, the hypothesis of Darwin [35] that the Moon separated off from the Earth and the giant-impact hypothesis [36] are not supported by

our results. A number of other theories in which the age of the Moon is substantially less than 4.5 billion years are likewise not supported. We have studied the evolution of the rotational motion of the Moon for the first time here. Our results suggest that the axial rotation of the Moon was initially opposite to its current direction. The current character of the Moon's motion developed several million years ago, when its rotation became prograde, it approached the Earth to a minimum distance, and then began to recede, entering into a 1 : 1 resonance at subsequent times.

Integrating the equations of motion into the future, we encountered an unrealistic time scale (due to the above comments concerning the coefficients k_1 and k_2), although the qualitative run of events is supported by theory [2, 3]. Based on this, we can express some events in terms of others. What should we be guided by in this case? Our theory yields a maximum distance between the Moon and Earth of 79.53, the theory of MacDonald [2] 72.5, and the theory of Goldreich [3] 75 Earth radii. These values are similar and realistic. Therefore, we expressed the remaining three variables in terms of the distance between the Moon and Earth, and represented the evolutionary picture into the future as a function of the radius of the lunar orbit and the recession from or approach toward the Earth. After reaching its maximum separation of 506 662 km, the Moon begins to approach the Earth. In the penultimate stage of the evolution, an unstable 1 : 1 : 1 synchronous resonance with the rotation of the Earth is added to the spin–orbit resonance of the Moon; this is then subsequently disrupted due to the sharp increase in the orbital angular velocity of the Moon. In the final stage, there is a close approach of the Moon toward the Earth ending with a collision. The same tidal-evolution mechanism is moving Phobos closer to Mars. Its orbital angular velocity, which is synchronized with its rotation, exceeds the rotational angular velocity of Mars by nearly a factor of three. This is what is predicted by our theory in the final stage of approach of the Moon and the Earth. According to the computations of Efroimsky and Lainey [8], Phobos will impact Mars in 40–43 million years. Deimos is currently receding from Mars, and it would be interesting to try to predict its evolution into the future.

In contrast to all the theories referred to above, we have considered the evolution not only of the orbital motion of the Moon, but also the evolution of the Earth–Moon barycenter. Tidal evolution led to an increase in the barycenter distance by 224 km. Based on an analysis of more than 635 000 observations of planets and spacecraft, primarily radio-technical data (1961–2010), Pit'eva and Pie'ev [37] derived the rate of variation of the heliocentric gravitational constant. Their results indicate that the barycenter of the Earth–Moon system is receding from the Sun at an average rate of 1 cm/year. Tidal evolution clearly makes a significant contribution to this process.

Thus, we conclude that our celestial-mechanical model with relatively few parameters is able to scientifically describe the tidal evolution of the Earth–Moon system over cosmological time intervals in a first approximation. The model does not include many physical processes, but nevertheless can provide qualitatively important results without invoking other complex theories. The most debatable issue is the origin of the Moon, which currently remains unresolved. The main conclusions given by our model are supported by astronomical observations, paleontological data, and studies based on other theories. We have also presented the possible evolution of the rotational motion of the Moon for the first time.

REFERENCES

1. G. H. Darwin, *The Tides and Kindred Phenomena in the Solar System* (CreateSpace Independent Publishing Platform, 2013; Nauka, Moscow, 1965).
2. G. J. F. MacDonald, Rev. Geophys. **2**, 467 (1964).
3. P. Goldreich, Rev. Geophys. **4**, 411 (1966).
4. V. V. Beletskii, Preprint Inst. Prikl. Matem. AN SSSR No. 43 (IPM AN SSSR, Moscow, 1978).
5. D. J. Webb, Geophys. J. R. Astron. Soc. **70**, 261 (1982).
6. G. A. Krasinsky, Celest. Mech. Dyn. Astron. **84**, 27 (2002).
7. J. Touma and J. Wisdom, Astron. J. **108**, 1943 (1994).
8. M. Efroimsky and V. Lainey, J. Geophys. Res.—Planets **112**, E12003 (2007).
9. F. Mignard, Moon Planets **20**, 301 (1979).
10. F. Mignard, Moon Planets **23**, 185 (1980).
11. S. Ferraz-Mello, A. Rodriguez, and H. Hussmann, Celest. Mech. Dyn. Astron. **101**, 171 (2008).
12. M. Efroimsky and J. G. Williams, Celest. Mech. Dyn. Astron. **104**, 257 (2009).
13. M. Efroimsky and V. V. Makarov, Astrophys. J. **764**, id. 26 (2013).
14. V. A. Churkin. Preprint Inst. Prikl. Astron. RAN No. 121 (IPA RAN, St.-Petersburg, 1998).
15. V. A. Churkin, Tr. Inst. Prikl. Astron. RAN, No. 4, 187 (1999).
16. V. A. Churkin, Tr. Inst. Prikl. Astron. RAN, No. 5, 225 (2000).
17. M. Efroimsky, Celest. Mech. Dynam. Astron. **112**, 283 (2012).
18. V. G. Vil'ke, *Analytical Mechanics of Systems with an Infinite Number of Degrees of Freedom* (Mekhmat MGU, Moscow, 1997) [in Russian].
19. V. G. Vil'ke, Prikl. Mat. Mekh. **44**, 395 (1980).
20. V. G. Vil'ke, S. A. Kopylov, and Yu. G. Markov, Prikl. Mat. Mekh. **49**, 25 (1985).
21. Yu. G. Markov and I. S. Minyaev, Astron. Vestn. **28**, 59 (1994).

22. V. G. Vil'ke and A. V. Shatina, Kosmich. Issled. **39**, 316 (2001).
23. A. A. Zlenko, *The Equations of Motion of Two Viscoelastic Spheres in the Central Force Field in the Double-Planet Problem* (Mosk. Avtodorozhn. Inst. (Gos. Tekh. Univ.), Moscow, 2009) [in Russian]; Available from VINITI RAN No. 581-V2009 (2009).
24. A. A. Zlenko, Kosmich. Issled. **49**, 569 (2011).
25. A. A. Zlenko, Kosmich. Issled. **50**, 490 (2012).
26. B. Luzum, N. Capitaine, A. Fienda, W. Folkner, T. Fukushima, J. Hilton, C. Hohenkerk, G. Krasinsky, G. Petit, E. Pitjeva, M. Soffel, and P. Wallace, Celest. Mech. Dyn. Astron. **110**, 293 (2011).
27. *Astronomical Year-Book 2012* (Nauka, St. Petersburg, 2011) [in Russian].
28. J. G. Williams and D. L. Boggs, in *Proceedings of the 16th International Workshop on Laser Ranging,* Ed. by S. Schillak (Space Res. Centre, Polish Acad. Sci., Warsaw, 2009), p. 101.
29. F. R. Stefenson and L. V. Morrison, Phil. Trans. R. Soc. A **351**, 165 (1995).
30. G. E. Williams, Geophys. Res. Lett. **29**, 421 (1997).
31. C. D. Murray and S. F. Dermott, *Solar System Dynamics* (Cambridge Univ. Press, Cambridge, 2000; Fizmatlit, Moscow, 2010).
32. G. A. Krasinsky, Soobshch. Inst. Prikl. Astron. RAN **148** (2002).
33. M. R. Walter, Science **170**, 1331 (1970).
34. W. M. Kaula, Rev. Geophys. Space **9**, 217 (1971).
35. G. H. Darvin, Phil. Trans. R. Soc. London **171**, 713 (1880).
36. W. K. Hartman and D. R. Davis, Icarus **24**, 504 (1975).
37. E. V. Pitjeva and N. P. Pitjev, Solar Syst. Res. **46**, 78 (2012).

Translated by D. Gabuzda